Food Chemistry: X 15 (2022) 100431

Contents lists available at ScienceDirect

Food Chemistry: X

journal homepage: www.sciencedirect.com/journal/food-chemistry-x

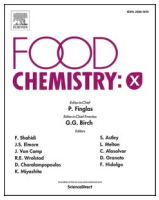

Delivery of curcumin by shellac encapsulation: Stability, bioaccessibility, freeze-dried redispersibility, and solubilization

Yongkai Yuan [a,b], Shuaizhong Zhang [a], Mengjie Ma [b], Ying Xu [a,*], Dongfeng Wang [a]

[a] College of Food Science and Engineering, Ocean University of China, Qingdao, Shandong Province 266003, People's Republic of China
[b] School of Food Science and Technology, Jiangnan University, Wuxi 214122, People's Republic of China

ARTICLE INFO

Keywords:
Encapsulation
Curcumin
Shellac
Nanoparticles

ABSTRACT

Curcumin is an active ingredient with multiple functions, however, its application is limited by its low stability, bioaccessibility, freeze-dried redispersibility, and solubilization. The work aims to improve the application of curcumin (Cur) by encapsulation. Shellac was the wall material inspired by its pH-dependent deprotonation and amphiphilic nature to form nanoparticles. The curcumin/shellac nanoparticles (S/Cur) exhibited a bright spot of high loading capacity (the maximum of higher than 70 %), while still having high encapsulation efficiency (the minimum of higher than 85 %). Transmission electron microscopy showed that S/Cur was a spherical structure. It exhibited good physical stability, including pH (4.0–8.0), ionic strength (NaCl, < 900 mM), thermo stability (80 ℃, 180 min), and storage stability (light and dark, 4 and 25 ℃, 20 days). Meanwhile, the chemical stability was increased by encapsulation. Furthermore, the bioaccessibility of Cur was improved to 75.95 %, which is attributed to the pH response of shellac. Additionally, S/Cur had freeze-dried redispersibility and solubilization, which is proportional to the mass ratio of shellac-to-Cur. The mechanism of S/Cur formation involved hydrophobic interaction and hydrogen bonds, and the nanoconfined Cur was amorphous.

1. Introduction

Curcumin (Cur) is an excellent active component, isolated from turmeric, which has attracted great attention due to its multiple functions, such as antioxidant, antitumor, and anti-inflammatory (Kocaadam & Sanlier, 2017; Liu et al., 2020). Currently, Cur is considered a new generation multifunctional drug and a nutritional fortifier in food (Lee, Loo, Young, Traini, Mason, & Rohanizadeh, 2014). However, the application of Cur is limited by its low water solubility, stability, and bioavailability. The construction of vectors is an effectual strategy to overcome the above-mentioned challenges, such as liposomes, emulsions, and nanoparticles (NPs) (Sanidad, Sukamtoh, Xiao, McClements, & Zhang, 2019). Biopolymer-based NPs have the characteristics of low fat, low energy consumption, small particle size, and high permeability (McClements, 2020; Yuan, Ma, Xu, & Wang, 2022). Particularly, natural materials have become the mainstream application considering the demand for "clean label" products (McClements & Gumus, 2016).

For the design of biopolymer-based NPs, it is necessary to consider the characteristics of both wall material and core material. Cur, as a hydrophobic core material, often requires organic reagents for dissolution, such as anti-solvent precipitation and anti-solvent co-precipitation (Sun et al., 2017; Yuan et al., 2020). These methods are limited by the flammability of organic reagents, the additional cost of removing organic reagents, and the application in organic solvent-free products (Sun, Gao, & Zhong, 2018; Yuan et al., 2021). It is worth noting that Cur can be dissolved under strongly alkaline conditions due to the deprotonation of –OH (Pan, Luo, Gan, Baek, & Zhong, 2014). Therefore, a low-energy pH cycle self-assembly without organic reagents was developed for the delivery of Cur. Specifically, this method is to increase the hydrophobicity of Cur by adjusting the pH of Cur dissolved in a strong alkali aqueous solution to neutral, while being encapsulated by the interactions with the wall material (Yuan, Ma, Xu, & Wang, 2021). Protein is usually used as the wall material for pH cycle self-assembly (Chen et al., 2021; Pan et al., 2014; Taghavi Kevij, Salami, Mohammadian, & Khodadadi, 2020; Zhan, Dai, Zhang, & Gao, 2020). However, the disadvantage of easy precipitation at the isoelectric point of the protein is inevitable. Thus, various stabilizers are selected to form a multi-composite system with protein, such as gliadin/rhamnolipid composite NPs (Chen et al., 2021), sodium alginate/sodium caseinate-coated zein NPs (Li et al., 2021), and sodium caseinate/fucoidan-coated zein NPs (Liu, Qin, Chen, Jiang, & Zhang, 2021), which undoubtedly increases the complexity of preparation and the cost of enterprise

* Corresponding author.
E-mail address: xuy@ouc.edu.cn (Y. Xu).

https://doi.org/10.1016/j.fochx.2022.100431
Received 10 June 2022; Received in revised form 3 August 2022; Accepted 12 August 2022
Available online 17 August 2022

production. Based on the principle of protein application in the pH cycle self-assembly, the hydrophobic structure of the wall material is important.

Shellac is a natural resin secreted by the female lac beetle, which has been recognized as safe by the Food and Drug Administration (FDA). In addition to the silk, architecture, and leather fields, the application of shellac has been extended to the pharmaceutical and food industry for its excellent enteric properties (Yuan et al., 2021a). For example, Zhou et al. (2021) designed a plant leaf-mimetic membrane with controllable gas permeation used for food preservation. Besides, Sun et al. (2017) reported zein/shellac composite colloidal particles fabricated by the antisolvent co-precipitation method for encapsulating and releasing Cur. Notably, shellac has a special structure, namely aleuritic acid and cyclic terpene acid connected by ester bond, and they are hydrophobic and hydrophilic respectively (Luo et al., 2016).

Inspired by the amphiphilic structure and pH-dependent deprotonation of shellac, we hypothesized that pH cycle encapsulation of Cur can be achieved using shellac. In this work, Cur-loaded shellac NPs (S/Cur) were fabricated by pH-driven self-assembly. The characterizations of S/Cur were evaluated systematically. And the potential of S/Cur applications was studied, including physicochemical stability, bioaccessibility (BA) during *in vitro* simulated gastrointestinal digestion (SGD), and dispersibility and solubilization after freeze-drying.

2. Materials and methods

2.1. Materials

Shellac was provided by Yunnan Zelin Forestry Technology Co., ltd (China). The others were purchased from Solarbio Co., ltd (China), including Cur, lecithin, pepsin, pancreatin, and bile salts.

2.2. Nano-encapsulation protocols

Under the conditions of 50 ℃ for 30 min, shellac was added to the water (pH 12.0). After the shellac solution was cooled to room temperature, Cur was added to it (pH 12.0) and stirred for 15 min until Cur was completely dissolved. Then, it was acidified to a pH of 7.0. The unencapsulated Cur was removed by centrifugation (3000 *g*, 10 min). The ratio of shellac-to-Cur was 1:5 to 5:1 (w/w), the codes of which were $S/Cur_{1:5}$ to $S/Cur_{5:1}$. The acid and base used were 1 M HCl and NaOH, respectively.

2.3. Dynamic light scattering and ζ-potential

Particle size and ζ-potential were measured with a ZS90 NANO-Malvern based on dynamic light scattering and capillary electrophoresis at 25 ℃.

2.4. Encapsulation efficiency and loading capacity

The encapsulation efficiency (EE) and loading capacity (LC) were determined according to our method that has been reported (Yuan et al., 2021b). In detail, 80 % ethanol was prepared to dilute nano-dispersion accompanied by ultrasound (20 min), and the data were obtained with a UV visible (426 nm) spectrophotometer. The presented values were calculated based on Eq. (1) and Eq. (2):

$$\mathrm{EE}\,(\%) = \frac{\text{encapsulated Cur (mg)}}{\text{total Cur (mg)}} \times 100\% \quad (1)$$

$$\mathrm{LC}\,(\%) = \frac{\text{encapsulated Cur (mg)}}{\text{total NPs (mg)}} \times 100\% \quad (2)$$

2.5. Morphology

The morphology of fresh S/Cur was detected by TEM (JEM-1400, Japan). Briefly, S/Cur was diluted appropriately using deionized water, one droplet of which was placed onto a copper film grid and dried with a lamp heating device. Then, the above-mentioned copper film grid was put into the TEM to start the detection.

2.6. Stability of nanoparticles

2.6.1. Physical stability

The pH values ranging from 2.0 to 8.0 were adjusted by adding HCl or NaOH to the fresh S/Cur for analysis of pH stability. For ionic strength stability, various masses of NaCl were added to S/Cur to give a final concentration of 0–1500 mM. S/Cur was heated at 80 ℃ for 180 min to study heating stability. Storage stability was carried out by storing S/Cur in transparent and brown glass bottles and placed at 4 and 25 ℃ respectively for 20 days. And the particle size and ζ-potential were used as evaluation indicators.

2.6.2. Chemical stability

During the storage as described in section 2.6.1, the chemical stability was investigated by the change of Cur content (C), which was determined as described in section 2.4. The retention rate (Rr) was calculated according to Eq. (3):

$$\mathrm{Rr}\,(\%) = \frac{C_{20days}}{C_{initial}} \times 100\% \quad (3)$$

2.7. In vitro SGD

A protocol of *in vitro* SGD was established referring to the international agreement (Minekus et al., 2014). The purpose is to appraise the BA of Cur and morphology tracking of NPs during this process. The simulated gastric fluid (SGF) and simulated intestinal fluids (SIF) composition are displayed in **Table S1**. NPs and SGF were mixed in equal volumes and shaken continuously in an incubator. The incubator conditions were 150 rpm, 37 °C, and 2 h. The same operation was taken during the intestinal phase. The BA was examined from the micellar phase (MP), which has been reported by our group (Yuan et al., 2021d). The BA was acquired according to Eq. (4):

$$\mathrm{BA}\,(\%) = \frac{C_{MP}}{C_{\mathrm{initial}}} \times 100\,\% \quad (4)$$

2.8. Redispersibility

Fresh S/Cur was freeze-dried (Christ Alpha 1-4LDplus, Christ, Germany) at −55 ℃ for 48 h. Then the S/Cur powder was dispersed in deionized water under stirring at 600 rpm for 20 min. The appearance of the redispersed S/Cur was observed and further analyzed by the particle size.

2.9. Solubilization after freeze-drying

The saturated solution of S/Cur, acquired by putting lyophilized S/Cur into deionized water continuously, was centrifuged (5199 *g*, 10 min) to acquire the Cur content in the supernatant, which was determined as described in section 2.4.

2.10. Infrared spectroscopy

An Infrared spectrometer (Nicolet IS3, Thermo, USA) was used to provide infrared information. The device parameters were 400 to 4000 cm^{-1}, 2 cm^{-1} resolution, and 64 scans. Thin slices were obtained by grinding and pressing the mixture of freeze-dried sample and potassium bromide with a ratio of 1:99 (w/w). The infrared spectra of pure

potassium bromide were set as the background of all samples.

2.11. X-ray diffraction (XRD)

An X-ray diffractometer (Bruker D8, Germany) was used to study crystalline information of Cur. The device parameters were 5° to 50° and 2°/min at an accelerating voltage of 40 kV and a tube current of 40 mA.

2.12. Statistical analysis

All experiments were carried out in triplicate separately. Results were expressed as means ± standard deviation (SD) and analyzed with one-way analysis of variance (ANOVA), followed by Tukey's test for multiple comparisons using SPSS. Differences between groups at $p < 0.05$ were considered statistically significant.

3. Results and discussion

3.1. Particle size, ζ-potential, encapsulation efficiency, loading capacity, and morphology

The construction evaluation of S/Cur was carried out by particle size, ζ-potential, EE, LC, and TEM. The different mass ratios of shellac to Cur were used to explore its influence on the possibility of constructing S/Cur to choose the best one for follow-up research. The particle size of S/Cur is shown in Fig. 1**A**. It could be seen that there was no notable difference ($p > 0.05$) between different groups, and the values were about 130 nm. Additionally, the values of absolute surface charges were higher than 30 mV (Fig. 1**B**). Generally, NPs solution with the value of absolute surface charges higher than 20 mV is considered to be a colloidally stable system (Moore & Cerasoli, 2010). Thus, each group was in a stable state under a wide range of ratios. In fact, no obvious large particles or precipitation were observed in our experiment. Interestingly, the absolute value of ζ-potential exhibited a decreasing trend with the increased mass of shellac, which is may be attributed to the composition changes of the S/Cur surface and the viscosity changes of the polar environment around the S/Cur (Ma et al., 2020).

In Fig. 1**C**, EE was enhanced within $S/Cur_{1:5}$ and $S/Cur_{1:1}$, implicating the insufficient shellac to encapsulate Cur (Peng et al., 2018b). When the proportion of shellac further increased, no difference ($p > 0.05$) for EE was within the groups, indicating more Cur molecules were entrapped in S/Cur. Notably, for our designed S/Cur, the EE was already as high as over 85 % even at the low ratio of shellac ($S/Cur_{1:5}$), showing outstanding encapsulation ability. Excitingly, the LC of $S/Cur_{1:5}$ was higher than 70 % (Fig. 1**D**). Additionally, it is normal for LC to gradually decrease with the increased shellac due to that the increase in the denominator was greater than that of the numerator according to Eq. (2).

In previous reported LC, block polymer with B6 peptide showed the Cur LC of 15.6 % (Fan et al., 2018). NPs composed of amine-functionalized silica exhibited the Cur LC of 9.75 % (Bolouki, Rashidi, Vasheghani-Farahani, & Piravi-Vanak, 2015). The 11 % LC of Cur-loaded β-lactoglobulin NPs was reported (Teng, Li, & Wang, 2014). Zein-dextran sulfate colloids, zein-chondroitin sulfate colloids and even zein-chondroitin sulfate-sophorolipid colloids all showed the Cur LC of<4 % (Liu et al., 2020; Yuan et al., 2020; Yuan et al., 2021c). Compared with these reports, S/Cur showed more prominent LC. This advantage may be attributed to the pH cycle self-assembly because this method has a higher Cur LC capability than the method containing organic reagents (Dai, Zhou, Wei, Gao, & McClements, 2019; Yuan et al., 2021b). However, the advantage of S/Cur is still obvious compared to other materials using the pH cycle self-assembly. For example, Cur vehicles composed of zein and rhamnolipid showed an LC of<14 % (Dai et al., 2019). Cur carriers consisting of zein and sophorolipid exhibited an LC of 11.50 % (Yuan et al., 2021b). The LC of Cur in zein/tea saponin was 22.33 % (Yuan et al., 2021d). The Cur LC within nano-encapsulation of gliadin and rhamnolipid was<10 % (Chen et al., 2021). Therefore, the high LC of S/Cur is not only due to the pH cycle self-assembly but also related to shellac. And pH cycle S/Cur exhibited high EE and LC at the same time. Based on the above discussion, $S/Cur_{1:1}$ was used for follow-up research. Meanwhile, the images of $S/Cur_{1:1}$ were shown in Fig. 1**E.** The formed NPs could be visually observed, showing a spherical structure. In addition, polyphenols are easily hydrolyzed in an alkaline environment, but Cur is only degraded by about 5 % for 1 h at pH 12.0 (Cheng et al., 2017), and the time we used was 15 min, thus the degradation rate of Cur was only about 1 %.

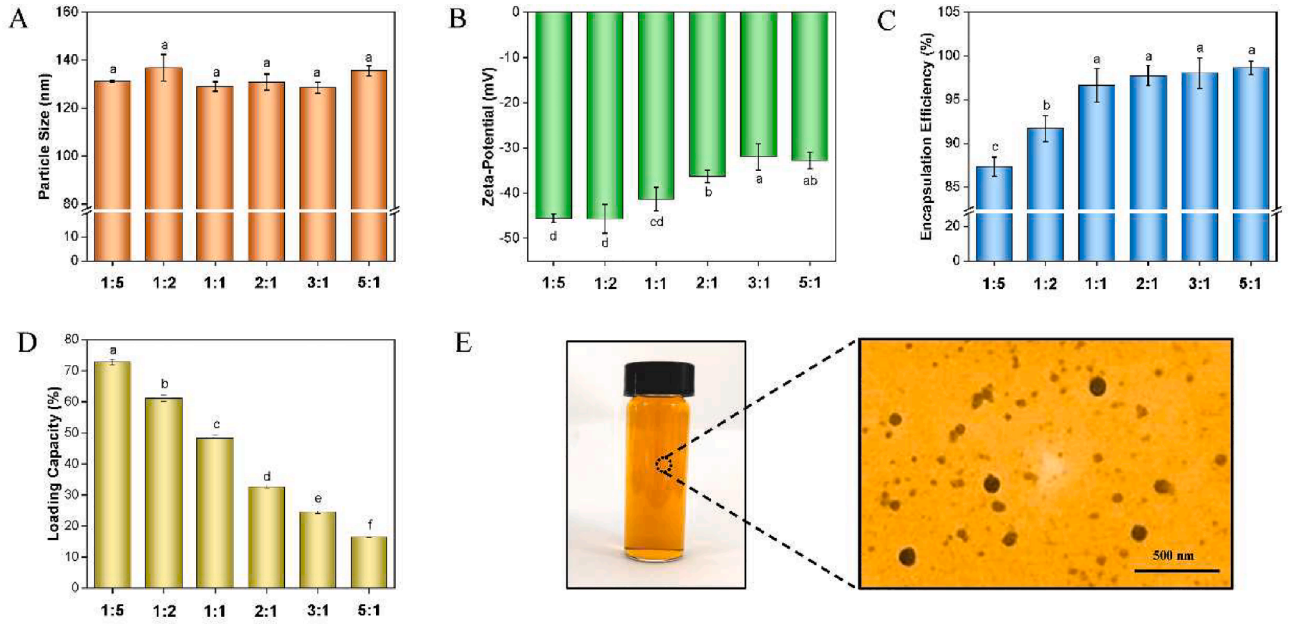

Fig. 1. Particle size (A), ζ-potential (B), encapsulation efficiency (C) and loading capacity (D) of S/Cur with different mass ratio of shellac to curcumin. (E) The appearance and TEM images of $S/Cur_{1:1}$. Data are expressed as the mean ± SD (n = 3). The different letters indicate the significant differences ($p < 0.05$) using Tukey's multiple comparisons.

3.2. pH stability

As illustrated in Fig. 2**A**, when the pH was higher than 4.0, the particle size was<150 nm, indicating the stability of nano-dispersion when the pH was higher than 4.0. However, the sizes of the samples with pH 2.0 and 3.0 increased significantly ($p < 0.05$) compared with pH > 4.0, suggesting instability in a strong acid environment. The reason was explored by ζ-potential. In Fig. 2**B**, S/Cur with pH > 4.0 exhibited high ζ-potential (green area), increasing the electrostatic repulsive force between NPs. But when the pH was lower than 4.0, the ζ-potential gradually approached zero, which means the electrostatic repulsive force between NPs was weakened, which is easy to cause aggregation. It has been reported that the stability of Cur-tea saponin-zein colloids, sophorolipid-zein and rhamnolipid-zein colloids fabricated by pH cycle was above pH 5 (Dai et al., 2019; Yuan et al., 2021b; Yuan et al., 2021d). Compared with these reported NPs, S/Cur with stability at pH 4.0–8.0 has a slight advantage.

3.3. Ionic strength stability

Considering the possibility of application in commodities and the human gastrointestinal environment, the effect of ionic strength on the stability of S/Cur was also pivotal. When the concentration of ions was < 900 mM, there was no difference markedly in sizes between groups (Fig. 2**C**), indicating excellent stability in terms of ionic strength. When the concentration was further increased (1200 mM and 1500 mM), the sizes increased markedly, which means the instability of S/Cur. The cause of instability is the electrostatic screening effect (Li et al., 2019). In

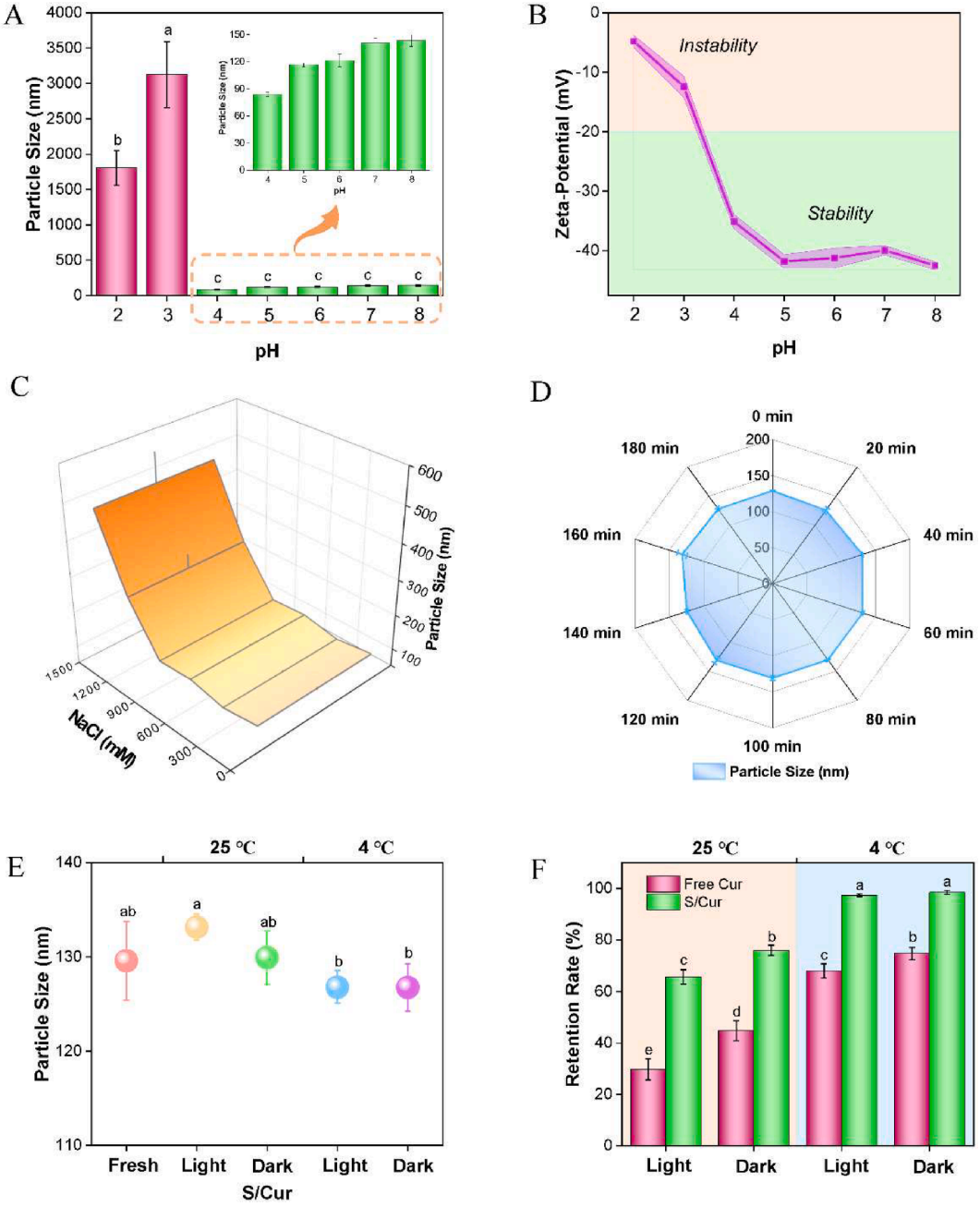

Fig. 2. Physicochemical stability of S/Cur. Effect of pH on the particle size (A) and ζ-potential (B). Effect of NaCl concentration (C) and heating at 80 ℃ (D) on the particle size. Effect of storage on the particle size (E) and retention rate of Cur (F). Data are expressed as the mean ± SD (n = 3). The different letters indicate the significant differences ($p < 0.05$) using Tukey's multiple comparisons.

previous studies, both pH cycle zein/rhamnolipid NPs and zein/tea saponin NPs showed ionic strength stability within 100 mM (Dai et al., 2019; Yuan et al., 2021d). pH cycle zein/sophorolipid colloids showed the stability of ionic strength within 250 mM (Yuan et al., 2021b). Both Cur-loaded sophorolipid NPs and saponin NPs prepared by pH cycle self-assembly exhibited ionic strength stability within 200 mM (Peng et al., 2018a; Peng et al., 2018b). Comparatively, S/Cur has excellent ionic strength stability.

3.4. Heating stability

Heating treatment in the production process of some commodities is necessary to achieve the desired flavor or sterilization. Thus, evaluating the effect of heating on the stability of S/Cur is critical. As observed in Fig. 2**D**, the particle size did not increase significantly within 180 min of heating at 80 ℃, indicating the good heating stability of S/Cur. A similar result was also found in pH cycle zein/tea saponin NPs, which had good thermostability at 80 ℃ for 150 min (Yuan et al., 2021d).

3.5. Storage stability

The storage effect of S/Cur was evaluated in different environments (light and dark, 4 and 25 ℃) for 20 days. As shown in Fig. 2**E**, regardless of the environment, the particle size did not increase significantly ($p > 0.05$), indicating excellent physical stability after the storage. The Cur Rr is displayed in Fig. 2**F**. It could be seen that the construction of nano-carriers distinctly ($p < 0.05$) improved the Rr of Cur, suggesting improved chemical stability during storage. Both light and temperature had a significant effect on the Rr of Cur. Refrigeration was beneficial to increase the Rr of Cur in S/Cur. The light-proof treatment provided by the brown bottle was beneficial to increase the Rr at room temperature. Interestingly, there was no distinct ($p > 0.05$) difference between the light and dark groups under refrigeration conditions. The enlightenment of these results for the S/Cur commercial applications is that it is best to use refrigerated storage. If stored at room temperature, it is recommended to use light-proof packaging, while it is not necessary to consider light-proof packaging when refrigerating.

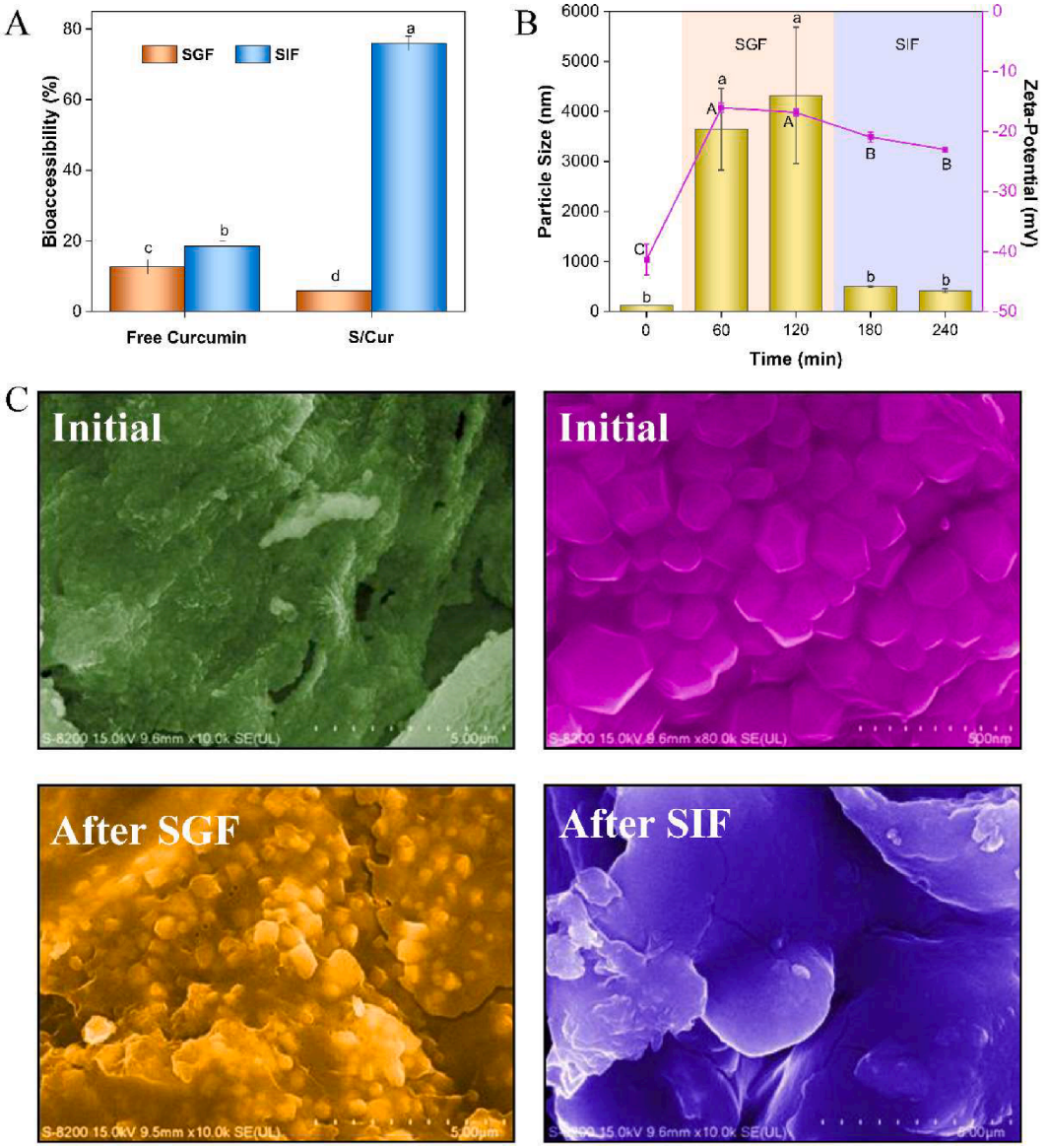

Fig. 3. (A) Bioaccessibility of Cur after SGF and SIF. Particle size, ζ-potential (B) and FE-SEM images (C) of S/Cur during SGF and SIF. SGF represents simulated gastric fluid. SIF represents simulated intestinal fluid. Data are expressed as the mean ± SD (n = 3). The different letters indicate the significant differences ($p < 0.05$) using Tukey's multiple comparisons.

3.6. Bioaccessibility

It is necessary to explore the impact of gastrointestinal digestion on the delivery system because the ultimate destination of the design of the carrier is to safely deliver nutrients to the small intestine to be used by the human body. The BA of Cur and the morphology of S/Cur were investigated during the SGD. In Fig. 3**A**, the BA of free Cur after SIF was<20 %, proving the low BA of free Cur. Interestingly, the BA of Cur in S/Cur was 75.95 % after SIF, and it was only 5.81 % after SGF. The results indicated the excellent controlled release ability of S/Cur, resulting in high BA after simulated digestion. To explain the high BA intuitively, the particle size, surface charges, and microstructure of the S/Cur were measured. Compared with the fresh S/Cur, the larger particle size and lower surface charges were measured after SGF (Fig. 3**B**), which is attributed to the pH/ions induced electrostatic repulsion decrease. In the subsequent SIF stage, enzymes/ions induced biopolymer destruction, leading to the opposite change of size and potential compared with that of SGF (Yuan et al., 2021c). In Fig. 3**C**, the appearance of the spherical particles of S/Cur before digestion could be observed clearly by FE-SEM. Obviously, these spherical particles still existed after SGF digestion. Although the S/Cur in the SGF stage exhibited a large particle size (Fig. 3**B**), it was the only agglomeration between particles and did not affect the Cur inside the particles, thereby protecting the Cur. However, the particles disappeared after SIF, which is attributed to the pH-response property of shellac (Yuan et al., 2021a). Thus, the encapsulated Cur was released, resulting in a high BA.

3.7. Redispersibility and solubilization after freeze-drying

Convenient for the storage, transportation, and carrying of commodities, freeze-drying is often used as a method to make commodities appear in solid form. The dispersibility and solubilization after freeze-drying are important criteria for evaluating the application possibilities of solid form. In Fig. 4**A**, the particle size of redispersed S/$Cur_{1:1}$ was significantly higher than that of fresh S/$Cur_{1:1}$, indicating S/$Cur_{1:1}$ did not have dispersibility. But in the experiment, we observed that S/$Cur_{1:1}$ was only partially no longer redispersed and there were a few large particles. This experimental phenomenon encouraged us to further investigate the influence of the proportion of shellac in NPs on dispersibility. Therefore, the dispersibility of S/$Cur_{5:1}$ was investigated. Interestingly, there was no difference remarkably ($p > 0.05$) in the size of S/$Cur_{5:1}$ before and after freeze-drying. The results indicated that S/$Cur_{5:1}$ had dispersibility, and the dispersibility of S/Cur was related to the mass ratio of shellac to Cur in NPs. The higher mass ratio of shellac contributed to the dispersibility of S/Cur. During the freeze-drying, the aggregation of NPs due to the capillary pressure effect was inevitable, which resulted in the decreased dispersibility of NPs (Wang, Zhang, Zhang, Mujumdar, & Huang, 2005). When the shellac in NPs had a high proportion, the aggregation tendency of S/Cur caused by the dehydration process could be suppressed by the protective effect of shellac, which is similar to the result of the Cur-loaded rhamnolipid NPs (Ma et al., 2020). The solubilization after freeze-drying is displayed in Fig. 4**B**. Cur exhibited extremely low water solubility, verifying that Cur is almost insoluble in water. However, both S/$Cur_{1:1}$ and S/$Cur_{5:1}$ remarkably ($p < 0.05$) increased the solubilization, and S/$Cur_{5:1}$ exhibited the better result, which is related to its dispersibility.

3.8. Interaction analysis

The interactions of S/Cur formation were explored by FTIR (Fig. 5**A**). For Cur, the stretching vibration (SV) of benzene ring phenolic hydroxyl (3509.94 cm^{-1}) could be found (Ma et al., 2020). There were no peaks in the range of 1800 cm^{-1} to 1650 cm^{-1}, which implied the keto-enol tautomerism form of Cur (Mangolim et al., 2014). Other peaks at 1628.01, 1603.51, 1510.77, and 1278.46 cm^{-1} were SV of carbon–carbon double bond and a carbon–oxygen double bond, carbon–carbon double bond in the benzene ring, carbon–carbon double bond and carbon–oxygen double bond vibrations, benzene ring SV of carbon–oxygen single bond (Hu et al., 2015). In addition, the peaks at 1151.64 and 811.01 cm^{-1} were C—C—H near the keto group (SV) and C—O—C near the inter-ring chain (SV) (Bich et al., 2009). Interestingly, both of them disappeared in the S/Cur spectrum, suggesting the hydrophobic interaction of Cur and shellac (Liang et al., 2015). For the spectrum of shellac, there was broadband at 3393.67 cm^{-1}, which means the O—H stretching vibration (Cerqueira, Souza, Teixeira, & Vicente, 2012). Notably, it shifted to 3431.32 cm^{-1} for S/Cur, implying the occurrence of hydrogen bonds. Therefore, the interactions in the formation of nano-dispersion involved hydrogen bonds and hydrophobic interaction.

3.9. Crystal analysis

In Fig. 5**B**, the pattern of Cur exhibited sharp peaks within the range of<30°, while shellac presented a flat peak. The results indicated the high crystallinity of Cur and the amorphous property of shellac. Interestingly, these sharp peaks disappeared after encapsulation. Notably, the physical blend of shellac and Cur still had the highly crystalline performance of Cur. Thus, the encapsulation turned Cur into amorphous, which may be due to the crystallization inhibition in the nano-confinement (Liang et al., 2015). Three additional peaks appeared in the pattern of S/Cur that assisted in proving the existence of noncovalent interactions during encapsulation. Li et al. also reported a similar result of soluble soybean polysaccharide-zein loaded with quercetin colloids

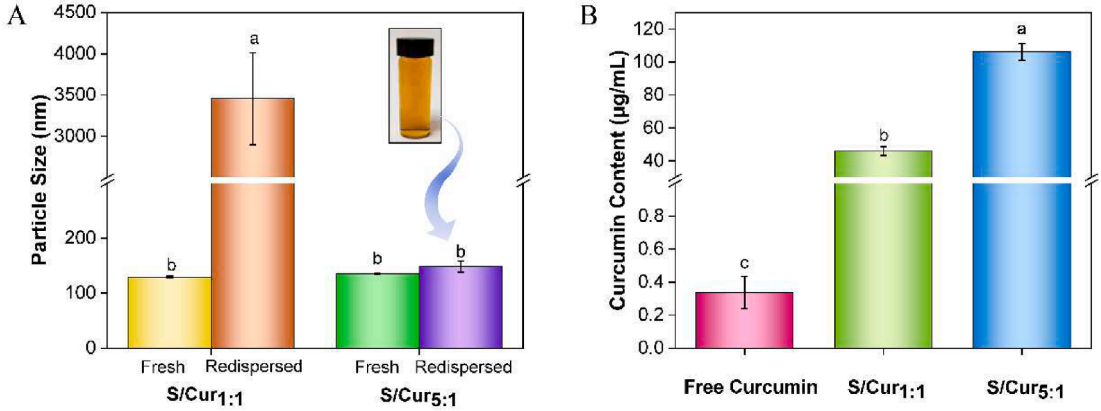

Fig. 4. (A) Particle size of freshly prepared and redispersed S/$Cur_{1:1}$ and S/$Cur_{5:1}$. The appearance of redispersed S/$Cur_{5:1}$ (inset of A). Solubilization of curcumin with or without encapsulation (B). Data are expressed as the mean ± SD (n = 3). The different letters indicate the significant differences ($p < 0.05$) using Tukey's multiple comparisons.

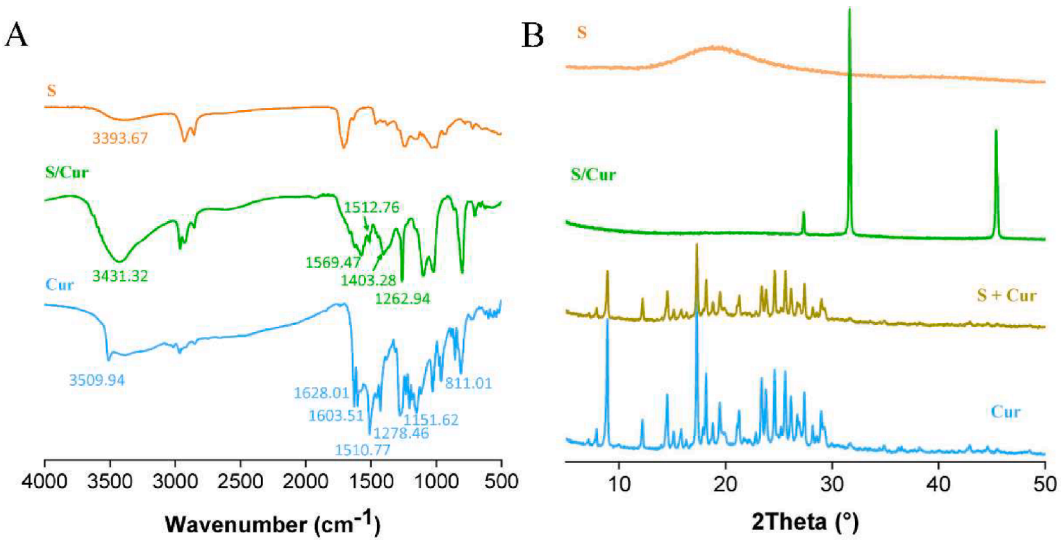

Fig. 5. FTIR (A) and XRD (B) of samples. S + Cur represents the physical mixture of shellac and curcumin.

(Li et al., 2019).

3.10. Construction mechanism

The construction mechanism of S/Cur was given in Fig. 6. Firstly, both shellac and Cur were in an alkaline environment based on the characteristics of alkali solubility of shellac and Cur. Then, HCl was used to introduce hydrogen ions to lower the pH to neutral. In this process, Cur regained hydrophobicity due to protonation, showing crystallization and avoiding the water environment. However, shellac has the hydrophobic group, which provides a place for hydrophobic Cur. Shellac and Cur were combined through the driving force of hydrophobic interaction and hydrogen bonds (supported by infrared spectroscopy) to form spherical nano-dispersion (supported by mean size/TEM) with an inner hydrophobic area and an outer hydrophilic area. Cur spontaneously accumulated in the hydrophobic area and had an amorphous nature due to nanoconfinement (supported by XRD). For the entire system, the high charge on the surface of the NPs provided strong electrostatic repulsion between the particles (supported by ζ-potential) and thus stable.

4. Conclusions

A novel NPs was constructed successfully only using a single wall material, that is shellac, to carry Cur by pH cycle. S/Cur has the advantages of low energy, organic solvent-free, and low cost, which is more suitable for enterprise applications. As far as the current Cur-loaded colloid systems are concerned, the high LC of S/Cur is a bright spot, while still having high EE. S/Cur exhibited good physical stability, including pH (4.0–8.0), ionic strength (NaCl, < 900 mM), thermostability (80 ℃, 180 min), and storage stability (light and dark, 4 and 25 ℃, 20 days). Meanwhile, the chemical stability was increased by encapsulation. Furthermore, the bioaccessibility of Cur was improved to 75.95 %, which is attributed to the pH response of shellac. Additionally, S/Cur had freeze-dried redispersibility and solubilization, which is proportional to the mass ratio of shellac-to-Cur. S/Cur has wide commercial application potential.

CRediT authorship contribution statement

Yongkai Yuan: Conceptualization, Methodology, Software, Writing – original draft, Data curation. **Shuaizhong Zhang:** Formal analysis, Investigation. **Mengjie Ma:** Formal analysis, Investigation. **Ying Xu:**

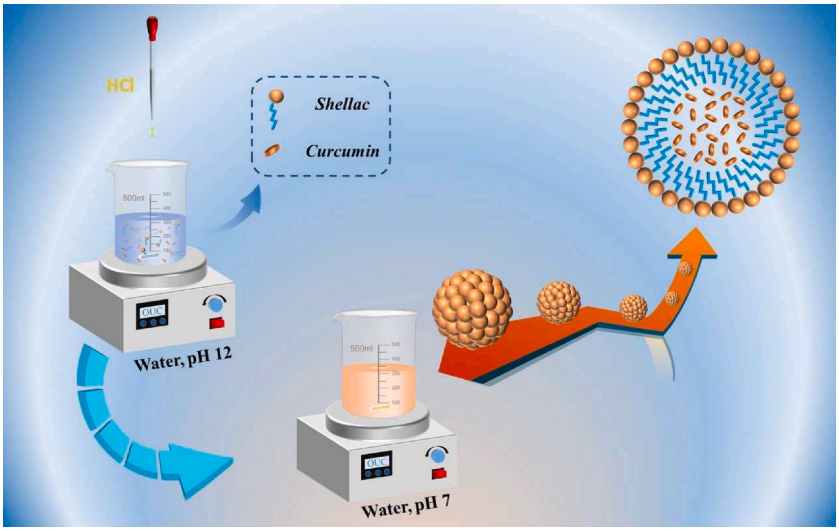

Fig. 6. Construction mechanism of curcumin-loaded shellac nanoparticles.

Supervision, Project administration, Funding acquisition, Writing – review & editing. **Dongfeng Wang:** Formal analysis, Investigation.

Declaration of Competing Interest

The authors declare that they have no known competing financial interests or personal relationships that could have appeared to influence the work reported in this paper.

Acknowledgements

This work was supported by the National Natural Science Foundation of China (Grant No. 31871786).

Appendix A. Supplementary data

Supplementary data to this article can be found online at https://doi.org/10.1016/j.fochx.2022.100431.

References

Bich, V. T., Thuy, N. T., Binh, N. T., Huong, N. T. M., Yen, P. N. D., & Luong, T. T. (2009). Structural and spectral properties of curcumin and metal-curcumin complex derived from turmeric (Curcuma longa). In *Physics and engineering of new materials* (pp. 271–278). Springer.

Bolouki, A., Rashidi, L., Vasheghani-Farahani, E., & Piravi-Vanak, Z. (2015). Study of Mesoporous Silica Nanoparticles as Nanocarriers for Sustained Release of Curcumin. *International Journal of Nanoscience and Nanotechnology, 11*(3), 139–146.

Cerqueira, M. A., Souza, B. W., Teixeira, J. A., & Vicente, A. A. (2012). Effect of glycerol and corn oil on physicochemical properties of polysaccharide films–A comparative study. *Food Hydrocolloids, 27*(1), 175–184.

Chen, S., Ma, Y., Dai, L., Liao, W., Zhang, L., Liu, J., & Gao, Y. (2021). Fabrication, characterization, stability and re-dispersibility of curcumin-loaded gliadin-rhamnolipid composite nanoparticles using pH-driven method. *Food Hydrocolloids, 118*, Article 106758.

Cheng, C., Peng, S., Li, Z., Zou, L., Liu, W., & Liu, C. (2017). Improved bioavailability of curcumin in liposomes prepared using a pH-driven, organic solvent-free, easily scalable process. *RSC Advances, 7*(42), 25978–25986.

Dai, L., Zhou, H., Wei, Y., Gao, Y., & McClements, D. J. (2019). Curcumin encapsulation in zein-rhamnolipid composite nanoparticles using a pH-driven method. *Food Hydrocolloids, 93*, 342–350.

Fan, S., Zheng, Y., Liu, X., Fang, W., Chen, X., Liao, W., … Liu, J. (2018). Curcumin-loaded PLGA-PEG nanoparticles conjugated with B6 peptide for potential use in Alzheimer's disease. *Drug Delivery, 25*(1), 1091–1102.

Hu, K., Huang, X., Gao, Y., Huang, X., Xiao, H., & McClements, D. J. (2015). Core-shell biopolymer nanoparticle delivery systems: Synthesis and characterization of curcumin fortified zein-pectin nanoparticles. *Food Chemistry, 182*, 275–281.

Kocaadam, B., & Sanlier, N. (2017). Curcumin, an active component of turmeric (Curcuma longa), and its effects on health. *Critical Reviews in Food Science and Nutrition, 57*(13), 2889–2895.

Lee, W.-H., Loo, C.-Y., Young, P. M., Traini, D., Mason, R. S., & Rohanizadeh, R. (2014). Recent advances in curcumin nanoformulation for cancer therapy. *Expert Opinion on Drug Delivery, 11*(8), 1183–1201.

Li, H., Wang, D., Liu, C., Zhu, J., Fan, M., Sun, X., … Cao, Y. (2019). Fabrication of stable zein nanoparticles coated with soluble soybean polysaccharide for encapsulation of quercetin. *Food Hydrocolloids, 87*, 342–351.

Li, Z., Lin, Q., McClements, D. J., Fu, Y., Xie, H., Li, T., & Chen, G. (2021). Curcumin-loaded core-shell biopolymer nanoparticles produced by the pH-driven method: Physicochemical and release properties. *Food Chemistry, 355*, Article 129686.

Liang, H., Zhou, B., He, L., An, Y., Lin, L., Li, Y., … Li, B. (2015). Fabrication of zein/quaternized chitosan nanoparticles for the encapsulation and protection of curcumin. *RSC Advances, 5*(18), 13891–13900.

Liu, C., Yuan, Y., Ma, M., Zhang, S., Wang, S., Li, H., … Wang, D. (2020). Self-assembled composite nanoparticles based on zein as delivery vehicles of curcumin: Role of chondroitin sulfate. *Food & Function, 11*(6), 5377–5388.

Liu, Q., Qin, Y., Chen, J., Jiang, B., & Zhang, T. (2021). Fabrication, characterization, physicochemical stability and simulated gastrointestinal digestion of pterostilbene loaded zein-sodium caseinate-fucoidan nanoparticles using pH-driven method. *Food Hydrocolloids, 119*, Article 106851.

Luo, Q., Li, K., Xu, J., Li, K., Zheng, H., Liu, L., … Sun, Y. (2016). Novel Biobased Sodium Shellac for Wrapping Disperse Multiscale Emulsion Particles. *Journal of Agricultural and Food Chemistry, 64*(49), 9374–9380.

Ma, Y., Chen, S., Liao, W., Zhang, L., Liu, J., & Gao, Y. (2020). Formation, Physicochemical Stability, and Redispersibility of Curcumin-Loaded Rhamnolipid Nanoparticles Using the pH-Driven Method. *Journal of Agricultural and Food Chemistry, 68*(27), 7103–7111.

Mangolim, C. S., Moriwaki, C., Nogueira, A. C., Sato, F., Baesso, M. L., Neto, A. M., & Matioli, G. (2014). Curcumin-beta-cyclodextrin inclusion complex: Stability, solubility, characterisation by FT-IR, FT-Raman, X-ray diffraction and photoacoustic spectroscopy, and food application. *Food Chemistry, 153*, 361–370.

McClements, D. J. (2020). Recent advances in the production and application of nano-enabled bioactive food ingredients. *Current Opinion in Food Science, 33*, 85–90.

McClements, D. J., & Gumus, C. E. (2016). Natural emulsifiers - Biosurfactants, phospholipids, biopolymers, and colloidal particles: Molecular and physicochemical basis of functional performance. *Advances in Colloid and Interface Science, 234*, 3–26.

Minekus, M., Alminger, M., Alvito, P., Ballance, S., Bohn, T., Bourlieu, C., … Brodkorb, A. (2014). A standardised static in vitro digestion method suitable for food - an international consensus. *Food & Function, 5*(6), 1113–1124.

Moore, J., & Cerasoli, E. (2010). Particle Light Scattering Methods and Applications. *Encyclopedia of Spectroscopy & Spectrometry*, 2077–2088.

Pan, K., Luo, Y., Gan, Y., Baek, S. J., & Zhong, Q. (2014). pH-driven encapsulation of curcumin in self-assembled casein nanoparticles for enhanced dispersibility and bioactivity. *Soft Matter, 10*(35), 6820–6830.

Peng, S., Li, Z., Zou, L., Liu, W., Liu, C., & McClements, D. J. (2018a). Enhancement of Curcumin Bioavailability by Encapsulation in Sophorolipid-Coated Nanoparticles: An in Vitro and in Vivo Study. *Journal of Agricultural and Food Chemistry, 66*(6), 1488–1497.

Peng, S., Li, Z., Zou, L., Liu, W., Liu, C., & McClements, D. J. (2018b). Improving curcumin solubility and bioavailability by encapsulation in saponin-coated curcumin nanoparticles prepared using a simple pH-driven loading method. *Food & Function, 9*(3), 1829–1839.

Sanidad, K. Z., Sukamtoh, E., Xiao, H., McClements, D. J., & Zhang, G. (2019). Curcumin: Recent Advances in the Development of Strategies to Improve Oral Bioavailability. *Annual Review of Food Science and Technology, 10*, 597–617.

Sun, C., Gao, Y., & Zhong, Q. (2018). Effects of acidification by glucono-delta-lactone or hydrochloric acid on structures of zein-caseinate nanocomplexes self-assembled during a pH cycle. *Food Hydrocolloids, 82*, 173–185.

Sun, C., Xu, C., Mao, L., Wang, D., Yang, J., & Gao, Y. (2017). Preparation, characterization and stability of curcumin-loaded zein-shellac composite colloidal particles. *Food Chemistry, 228*, 656–667.

Taghavi Kevij, H., Salami, M., Mohammadian, M., & Khodadadi, M. (2020). Fabrication and investigation of physicochemical, food simulant release, and antioxidant properties of whey protein isolate-based films activated by loading with curcumin through the pH-driven method. *Food Hydrocolloids, 108*, Article 106026.

Teng, Z., Li, Y., & Wang, Q. (2014). Insight into curcumin-loaded beta-lactoglobulin nanoparticles: Incorporation, particle disintegration, and releasing profiles. *Journal of Agricultural and Food Chemistry, 62*(35), 8837–8847.

Wang, B., Zhang, W., Zhang, W., Mujumdar, A. S., & Huang, L. (2005). Progress in Drying Technology for Nanomaterials. *Drying Technology, 23*(1–2), 7–32.

Yuan, Y., He, N., Xue, Q., Guo, Q., Dong, L., Haruna, M. H., … Li, L. (2021). Shellac: A promising natural polymer in the food industry. *Trends in Food Science & Technology, 109*, 139–153.

Yuan, Y., Huang, J., He, S., Ma, M., Wang, D., & Xu, Y. (2021). One-step self-assembly of curcumin-loaded zein/sophorolipid nanoparticles: Physicochemical stability, redispersibility, solubility and bioaccessibility. *Food & Function, 12*(13), 5719–5730.

Yuan, Y., Li, H., Zhu, J., Liu, C., Sun, X., Wang, D., & Xu, Y. (2020). Fabrication and characterization of zein nanoparticles by dextran sulfate coating as vehicles for delivery of curcumin. *International Journal of Biological Macromolecules, 151*, 1074–1083.

Yuan, Y., Ma, M., Xu, Y., & Wang, D. (2021). Construction of biopolymer-based nanoencapsulation of functional food ingredients using the pH-driven method: A review. *Critical Reviews in Food Science and Nutrition*, 1–15.

Yuan, Y., Ma, M., Xu, Y., & Wang, D. (2022). Surface coating of zein nanoparticles to improve the application of bioactive compounds: A review. *Trends in Food Science & Technology, 120*, 1–15.

Yuan, Y., Ma, M., Zhang, S., Liu, C., Chen, P., Li, H., … Xu, Y. (2021). Effect of sophorolipid on the curcumin-loaded ternary composite nanoparticles self-assembled from zein and chondroitin sulfate. *Food Hydrocolloids, 113*, Article 106493.

Yuan, Y., Xiao, J., Zhang, P., Ma, M., Wang, D., & Xu, Y. (2021). Development of pH-driven zein/tea saponin composite nanoparticles for encapsulation and oral delivery of curcumin. *Food Chemistry, 364*, Article 130401.

Zhan, X., Dai, L., Zhang, L., & Gao, Y. (2020). Entrapment of curcumin in whey protein isolate and zein composite nanoparticles using pH-driven method. *Food Hydrocolloids, 106*, Article 105839.

Zhou, Z., Ma, J., Li, K., Zhang, W., Li, K., Tu, X., … Zhang, H. (2021). A Plant Leaf-Mimetic Membrane with Controllable Gas Permeation for Efficient Preservation of Perishable Products. *ACS Nano, 15*(5), 8742–8752.